PA07-070

Study of muon-pair production at centre-of-mass energies from 20 to 136 GeV with the ALEPH detector.

Preliminary

The ALEPH collaboration

Abstract

The total cross section and the forward-backward asymmetry for the process $e^+e^- \to \mu^+\mu^-(n\gamma)$ are measured in the energy range 20-136 GeV by reconstructing the effective centre-of-mass energy after Initial State Radiation. The analysis is based on the data recorded with the ALEPH detector at LEP between 1990 and 1995, corresponding to a total integrated luminosity of 143 pb^{-1}. Two different approaches are used: in the first one an exclusive selection of events with hard Initial State Radiation in the energy range 20-88 GeV is directly compared with the Standard Model predictions showing good agreement. In the second one, all events are used to obtain a precise measurement of the energy dependence of σ^μ and A^μ_{FB} from a model independent fit, enabling constraints to be placed on models with extra Z bosons.

(Paper contributed to Warsaw Conference, July 1996)

1 Introduction

The muon cross section and forward-backward asymmetry have been accurately measured at different energy points around the Z mass [1]. These measurements allow a precise determination of the effective couplings of the Z to muons. Once the vector and axial coupling are measured, together with the known photon couplings, they determine the complete behaviour of the cross section and forward-backward asymmetry at any other energy if no new physics beyond the Standard Model is present.

In a more general framework, however, the description of the energy dependence of these quantities requires the introduction of new additional parameters which, with the present measurements, can be determined at LEP only with limited accuracy.

In practice, by using a structure function representation for the initial electron and positron, we know that the cross section measurements are a centre-of-mass average of the actual "hard scattering" cross sections. Conceptually, the Initial State Radiation energy losses are effectively "scanning" (although in a very non-uniform way) the "hard scattering" process in a range of energies much broader than the nominal LEP one.

Since we assume that QED is a well established theory which allows very accurate calculations of such radiation probability, we know how this "ISR scan" is performed. Thus we can derive from the data the probability for the "naked beams" to collide at a certain energy. The idea, then, is trying to be more "exclusive" in the measurements, extracting from the event characteristics the centre-of-mass energy of the "hard scattering" process. Although this is not a rigorous statement in quantum mechanics, we shall see that theoretically one can, with very good approximation, justify its validity.

So far, the analysis of radiative muon events carried out by other experiments [2] has been based on the specific selection of events with strong Initial State Radiation. This approach has been followed and the results compare well with the Standard Model (SM) expectations.

However, going one step further, a more general method to determine, on an event-by-event basis, the actual centre-of-mass energy of the "hard scattering" process has been developed. This approach allows the use of all muon events and hence, the whole statistical power of the data, maximizing the sensitivity to the S-matrix parameters [3]. A precise determination of the cross section and the forward-backward asymmetry over a wide range of energies is obtained. These measurements enable accurate determinations of the energy dependence of the cross section and forward-backward asymmetry to be made as well as the existence of new Z bosons to be constrained.

The outline of this paper is the following: in section 2 we analyze the theoretical justification of our new approach. Section 3 is devoted to the discussion of the event selection, and of the two analysis methods. In section 4 the results and a summary

of the main systematic uncertainties are presented. Finally in sections 5 and 6, limits on extra Z bosons and conclusions are given.

2 Theoretical formalism

The probability density that describes the process $e^+e^- \to \mu^+\mu^-(n\gamma)$ at a given centre-of-mass energy ($\sqrt{s}$), can be written as:

$$\begin{aligned} \frac{d^2\sigma}{dx d\cos\theta}(s) &= H(s,x)\left[\frac{3}{8}(1+\cos^2\theta)\sigma_T^0(s') + \cos\theta\sigma_{FB}^0(s')\right] \\ s' &\equiv s(1-x) \end{aligned} \tag{1}$$

Here θ is the scattering angle in the centre-of-mass of the hard process, and s' is the square of the modulus of the 4-momentum of the intermediate boson (γ or Z), x being the fraction of radiated energy. All the electroweak radiative corrections, Z and γ vacuum polarization, vertex and box corrections are absorbed in the definition of σ_T^0 and σ_{FB}^0 , while $H(s,x)$ is the radiator function that accounts for QED bremsstrahlung corrections.

One can think of $\sqrt{s'}$ as the "effective" centre-of-mass energy after Initial State Radiation (ISR). Of course, this interpretation is only valid if the interference between Initial and Final State Radiation (I-F) can be neglected. This is, in general, the case at the Z pole for inclusive observables where no strong cuts on the phase space of the final state particles are applied. It is not, however, true when the variable s' (or x) in (1) is not integrated. Moreover, I-F QED interference also distorts the angular distribution of (1). To avoid these effects, instead of using the differential expression given in (1), the x-distribution is binned in intervals wide enough to be as insensitive as possible to them, and $\Delta x \sim 0.04$ is chosen as a reasonable compromise for the bin size. This corresponds to a bin size of the order of the Z width which, somehow, separates physically the initial and final state wavefunctions and hence the effect of the interference is small, at the price of being less exclusive.

On the other hand, the probability density (1) is only well defined ($\frac{d^2\sigma}{dx d\cos\theta}(s) > 0$) for all values of $\cos\theta$, when $\mid \sigma_{FB} \mid < \frac{3}{4}\sigma_{TOT}$. This is a consequence of the fact that the helicity amplitudes that build it need to be positive defined. This is not a problem when the measured asymmetry is far from this theoretical constraint, but would introduce strong correlations between the fitted parameters when it is close to it as is the case at $\sqrt{s'} \sim 80$ GeV or $\sqrt{s'} \sim 113$ GeV (see for instance [6]). In order to overcome this problem, the angular distribution is also binned in two regions defined by $\cos\theta \geq 0$ (forward hemisphere) and $\cos\theta < 0$ (backward hemisphere). This is equivalent to computing the forward-backward asymmetry counting the events in both hemispheres, and consequently not imposing any hypothesis on the angular distribution of these events.

Therefore, the probability density for an event being in the interval $x_i \leq x < x_{i+1}$

will be given by:

$$P(x_i, \cos\theta_i, s) \equiv \frac{1}{2}\int_{x_i}^{x_{i+1}} dx H(s,x)(\sigma_T^0(s,x) \pm \sigma_{FB}^0(s,x)) \quad (2)$$

where the positive sign corresponds to the case $\cos\theta \geq 0$ and the negative sign to the case $\cos\theta < 0$.

The simplest S-Matrix [3] parameterization for the process $e^+e^- \to \mu^+\mu^-$ predicts the total and the forward-backward cross section as

$$\sigma_T^0 = \frac{4}{3}\pi\alpha^2 \left[\frac{g_\mu^{tot}}{s} + \frac{s\mathbf{r_\mu^{tot}} + (\mathbf{s} - \overline{\mathbf{M}}_\mathbf{Z}^\mathbf{2})\mathbf{j_\mu^{tot}}}{(s - \overline{\mathbf{M}}_\mathbf{Z}^\mathbf{2})^\mathbf{2} + \overline{\mathbf{M}}_\mathbf{Z}^\mathbf{2}\overline{\mathbf{\Gamma}}_\mathbf{Z}^\mathbf{2}}\right] \quad (3)$$

$$\sigma_{FB}^0 = \frac{4}{3}\pi\alpha^2 \left[\frac{s\mathbf{r_\mu^{fb}} + (\mathbf{s} - \overline{\mathbf{M}}_\mathbf{Z}^\mathbf{2})\mathbf{j_\mu^{fb}}}{(s - \overline{\mathbf{M}}_\mathbf{Z}^\mathbf{2})^\mathbf{2} + \overline{\mathbf{M}}_\mathbf{Z}^\mathbf{2}\overline{\mathbf{\Gamma}}_\mathbf{Z}^\mathbf{2}}\right] \quad (4)$$

The forward-backward asymmetry is given by

$$A_{FB} = \frac{\sigma_{FB}^0}{\sigma_T^0} \quad (5)$$

Assuming that the photon exchange parameter g_μ^{tot} is known from QED, (as it has been done for the radiator function H(s,x)), then the simplest S-matrix parameterization requires 6 parameters:

$$\overline{M}_Z, \overline{\Gamma}_Z, r_\mu^{tot}, j_\mu^{tot}, r_\mu^{fb}, j_\mu^{fb}$$

There is a simple relation between $\overline{M}_Z$, $\overline{\Gamma}_Z$ and the usual definitions of the Z mass and width:

$$\begin{aligned} M_Z &= \overline{M}_Z\sqrt{(1 + \overline{\Gamma}_Z^2/\overline{M}_Z^2)} \\ \Gamma_Z &= \overline{\Gamma}_Z\sqrt{(1 + \overline{\Gamma}_Z^2/\overline{M}_Z^2)} \end{aligned} \quad (6)$$

which corresponds to a shift in M_Z of 34 MeV and in Γ_Z of 0.9 MeV.

3 Event selection

As mentioned in the introduction, two different approaches have been followed. In both cases, the selection of dimuon events starts from the standard cuts applied in previous ALEPH [1] analyses to identify muon pair candidates, except that no cut on acollinearity or particle momentum is applied.

In order to study the effect of the experimental cuts, more than 2×10^6 events have been generated and fully reconstructed through a detector simulation, using the DYMU3 [4] and KORALZ 4.0 [5] (for the inclusive approach) Monte Carlo generators at several nominal LEP energies. The latter treats the radiation of hard

photons in the initial and final state to $\mathcal{O}(\alpha^{\in})$ and the former only to $\mathcal{O}(\alpha)$. In the case of KORALZ the radiation of soft photons is considered at all orders by exponentiation.

To reconstruct the effective centre-of-mass energy ($\sqrt{s'}$), it is considered that the only effect of the initial-state photon radiation is to boost the centre-of-mass system along the beam direction, (i.e. the photons are emitted in that direction). In this approximation the radiated energy E_{γ}^{ISR} can be computed from the measured directions of the final state particles.

The boost , $\beta = \frac{V}{c}$, that relates the LAB system and the CM system determines the radiated energy along the beam pipe through:

$$E_{\gamma}^{ISR} = \frac{\mid \beta \mid}{1+ \mid \beta \mid}\sqrt{s} \tag{7}$$

where $\sqrt{s}$ is the nominal centre-of-mass energy.

In the case where there is no FSR, both particles will be back-to-back in the CM system. This condition determines β as a function of the measured polar angles of the two muon candidates (θ_1 and θ_2) through:

$$\mid \beta \mid = \frac{\mid \sin(\theta_1 + \theta_2) \mid}{\sin\theta_1 + \sin\theta_2} \tag{8}$$

If one considers also the possibility to have one radiated photon in the final state, the three particles ($\mu^+\mu^-\gamma_{FS}$) will be contained in a plane in the CM system. So, from the relative angles measured in the LAB system, θ_{ij}, one can compute β such that the angles in the CM system, θ'_{ij} satisfy the condition that defines a plane. In this case, one can only solve numerically the equation to find β. Once β is known, s' is determined through:

$$x = \frac{2 \mid \beta \mid}{1+ \mid \beta \mid} \tag{9}$$

The only limitations come from the experimental precision on the measurements of the directions of the detected particles, and from the error induced by the ISR collinear approximation. The resolution on x is very good; as can be observed in fig. 1, the RMS of the differences between the reconstructed (x_{rec}) and generated (x_{gen}) radiated energy is around 0.01.

3.1 Selection of dimuon events with hard ISR

In the first analysis, an exclusive selection of dimuon events with hard ISR is performed. The process allows a clear separation between photons and the outgoing leptons, and hence gives a good rejection of the final-state bremsstrahlung events. The effective centre-of-mass energy $\sqrt{s'}$ is computed with (8), and only events in the range 20 GeV $< \sqrt{s'} <$ 88 GeV are analyzed.

Both muon candidates are required to have an energy of at least 10 GeV and a total energy greater than 45 GeV. In order to eliminate the remaining tau background and FSR dimuon events, the following cuts as a function of the reconstructed s' have been applied:

- $\sqrt{s'}$ - $M_{\mu\mu} < C_1(s')$, $M_{\mu\mu}$ being the invariant mass of the two muon candidates.
- $N_\gamma < 2$ and $|\cos(\theta_\gamma)| > C_2(s')$
- acoplanarity $< C_3(s')$
- missing $\mathrm{P_T} < C_4(s')$

The values of the cuts C_i for each bin are given in table 1. Data from the years 92 to 95 corresponding to a total luminosity of 138 pb^{-1} are used. A total of 986 dimuon events are selected compared to 1026.7 expected from Monte Carlo simulation (normalized to the same luminosity), with 25 of the events coming from two photon background. The results of this direct comparison with the MC predictions are shown in table 2.

3.2 Inclusive selection

In this case, no specific selection of hard ISR events is made, and the only requirements added to the standard muon selection are:

- p1 $> 35\ \frac{\sqrt{s}}{91.2}$, p1 being the momentum of the most energetic track.
- $N_\gamma < 2$, i.e., only one object in the EM calorimeter with more than 0.3 GeV.
- $(E_\gamma^{FSR} - ECAL) < 4\sigma$, E_γ^{FSR} being the energy of the FSR photon determined from the kinematics of the event, and ECAL the associated signal in the EM calorimeter.
- $(\sqrt{s} - E_\gamma^{ISR}) - (p_{\mu^+} + p_{\mu^-} + ECAL) < 4\sigma$, E_γ^{ISR} being the energy computed with (7).

The first cut, eliminates completely the two photon background. The last cut requires the total energy to be conserved, and gets rid of the remaining tau background. The only remaining background is misidentified Bhabhas (0.09%). The total efficiency of the selection of dimuon candidates is $(80.34 \pm 0.05)\%$ at the Z peak.

The probability density (2) needs to be corrected for the experimental efficiency as a function of (x_{rec}). The efficiency in both hemispheres in the interval $x_i \leq x < x_{i+1}$, $(\epsilon^i_{F,B})$, is expected to be different due to the fact that $A_{FB} \neq 0$ at $x \neq 0$, and the angular acceptance is restricted to $|\cos\theta| < 0.9$. Moreover, there is a kinematic effect when $x \neq 0$ due to the boost of the centre-of-mass system that reduces the efficiency inside the angular acceptance.

The qualitative picture of these efficiency functions does not change with $\sqrt{s}$. Nevertheless, they have been computed for all the different LEP nominal energy points.

4 Results and systematic studies

The data sample used in the inclusive analysis was recorded in the years 1990 to 1995 at centre-of-mass energies from 88.2 up to 136.2 GeV, and corresponds to a total integrated luminosity of 143.5 pb^{-1}. A total of 130,233 events pass the selection cuts.

The probability density of (2) corrected for the experimental efficiency at each energy point, is used to build a normalized log-likelihood function defined as the sum of the logarithms of the single-event probabilities. These probabilities are convoluted with a "gaussian" probability density due to the beam energy spread. The residual effect due to the I-F QED interference on σ^0_{FB} is taken into account, with an analytic expression that computes such corrections to $\mathcal{O}(\alpha)$.

The total normalization of the probability density is used as a new constraint (χ^2_1), together with the experimental measurements of M_Z and Γ_Z (χ^2_2), determined from the hadronic lineshape [7], ($M_Z = 91.2027 \pm 0.0077$ GeV and $\Gamma_Z = 2.4935 \pm 0.0058$ GeV), so that, with the above constraints, the final function to be minimized is:

$$l \;=\; -2 \sum_{i=1,N_{evt}} \ln\left(\hat{P}(x_i, \cos\theta_i, s)\right) + \chi^2_1 + \chi^2_2 \qquad (10)$$

The results obtained are shown in table 4 together with the SM predictions. The χ^2 of the fit is $\frac{\chi^2}{d.o.f.} = \frac{204.1}{187}$ corresponding to a confidence level of 18.6%.

The results are in perfect agreement with the SM, and the statistical precision of the measurements of j^{tot}_μ and j^{fb}_μ is now about two times better than the previous measurement in ALEPH [7] and is of similar precision than the LEP average.

A direct comparison with the predictions of the fit as a function of the $\sqrt{s'}$ interval is shown in table 3.

One can also define σ^0 and A^0_{FB} as:

$$\begin{aligned}
\sigma^0_F(<\sqrt{s'}>) &\equiv \sigma^{fit}_F(<\sqrt{s'}>)\frac{N^{obs}_F}{N^{fit}_F} \\
\sigma^0_B(<\sqrt{s'}>) &\equiv \sigma^{fit}_B(<\sqrt{s'}>)\frac{N^{obs}_B}{N^{fit}_B}
\end{aligned}$$

$$\begin{aligned}
\sigma^0 &= \sigma^0_F + \sigma^0_B \\
\sigma^0_{FB} &= \sigma^0_F - \sigma^0_B
\end{aligned}$$

Consequently, a measurement of the total cross-section and forward-backward asymmetry is obtained over a wide range of energies, where the effect of the ISR has

been deconvoluted. The results of this exercise are shown in tables 6 and 5 for the exclusive and inclusive analyses. In fig. 2 and fig. 3 one can compare also these measurements with previous measurements made at PEP [8], PETRA [9] and TRISTAN [10] at lower energies. The low energy data from these experiments are corrected to include the effect of the running of the fine structure constant, α.

Different sources of possible systematic errors on the measured S-matrix parameters have been investigated:

- The statistical uncertainty due to the finite number of MC events used to determine $\epsilon^i_{F,B}$, has been propagated in the fit, and the error is quoted in table 7.
- The uncertainty associated with the calculation to $\mathcal{O}(\alpha)$ of the I-F QED interference corrections. This has been evaluated from the data itself comparing the change on the asymmetry after a cut on the radiated energy, with the one predicted by the analytic calculation. A discrepancy of $\sim 70\%$ is observed, and propagated to the S-matrix parameters as shown in table 7.
- The limitations of the MC simulation to reproduce the angular distribution of hard photons emitted in the FS at large angles with respect the muon direction. The effect of cutting these events on the EW parameters has been quoted as systematic errors in table 7.
- The effect of the remaining Bhabha background has also been considered as a systematic error in table 7.
- The uncertainty on the beam energy spread has been propagated in the fit, and the effect is quoted in table 7.

5 Limits on extra Z bosons

Despite the excellent performance of the SM so far, there is a general consensus that it is not the "final" theory. Most of the attempts to unify the strong and electroweak interactions predict additional neutral heavy gauge bosons Z'. New interference terms, such as $\gamma - Z'$ and $Z - Z'$ will appear at the Born level and will modify the cross-section and angular distribution at energies far from $\sqrt{s} \sim M_Z$.

After specifying the model (and without any assumption on the structure of the Higgs sector), only two free parameters remain: i) the mixing angle θ_3 between Z and Z', ii) the mass of the heavier-mass eigenstate, $M_{Z'}$.

To obtain exclusion limits, a χ^2 has been computed comparing the values that appear in table 6 with different theoretical models. The ALEPH measurements of the hadronic cross section reported in [11] have also been included, but they only improve the sensitivity to the mixing angle.

Four of the most popular models that introduce a new Z boson have been considered. Three of them (χ-model, ψ-model and η-model) are superstring-inspired

models based on the E_6 symmetry group. The other one is a left-right symmetric model that includes a right-handed $SU(2)_R$ extension of the Standard Model gauge group $SU(2)_L \otimes U(1)$. These kind of models are characterized by the parameter α_{L-R} that describes the coupling of the Z' to fermions. The specific value $\alpha_{L-R} = 1$ has been chosen.

The effects of the Z' for the L-R and E_6 models on the cross sections and asymmetries have been calculated using an addition to the ZFITTER program, called ZEFIT (vers. 3.1) [12], that provides radiatively corrected cross sections and asymmetries for the process $e^+e^- \to f\bar{f}$. As the standard Z^0 mass changes due to the presence of a mixed Z', M_Z was also fitted (using the direct M_Z measurement constraint) along with the mixing angle θ_3 and the Z' mass.

The region defined by $\chi^2 < \chi^2_{min} + 5.99$ correspond to 95% confidence level for one sided exclusion bounds for two parameters. This is plotted in fig. 4 for the models considered, and in table 8 one can explicitly see the limits. In the same fig. 4 one can see the exclusion limits published by CDF [13], in a direct search of new produced Z' bosons.

6 Conclusions

An exclusive selection of hard Initial State Radiation events has been performed. A total of 986 events are selected, and good agreement with the Standard Model expectations is observed at centre-of-mass energies between 20 and 88 GeV.

Going one step further, the full statistical power of the event sample has been used by reconstructing, for all events, the effective centre-of-mass energy $\sqrt{s'}$ on an event-by-event basis. A precise measurement of the total cross section and the forward-backward asymmetry in a range of energies still uncovered by present accelerators, extending from 60 up to 136 GeV, has been performed. As a result, the EW parameters that describe, in a general way, the energy dependence of these observables are determined with an unprecedented precision equivalent to the one obtained by the four LEP experiments together using the standard analysis described in [7].

The results obtained for the S-matrix EW parameters are:

$$\begin{aligned} r_\mu^{tot} &= 0.14201 \pm 0.00084 \pm 0.00005 \\ j_\mu^{tot} &= -0.017 \pm 0.020 \pm 0.007 \\ r_\mu^{fb} &= 0.00272 \pm 0.00054 \pm 0.00037 \\ j_\mu^{fb} &= 0.804 \pm 0.024 \pm 0.014 \end{aligned}$$

The improved precision on the measured energy dependence, specially the energy dependence of the forward-backward asymmetry j_μ^{fb}, allows the existing limits from LEP for $M_{Z'}$ to be improved. The sensitivity to the mixing angle θ_3 is determined by the existing measurements at the Z peak.

Acknowledgments

It is a pleasure to thank our colleagues in the accelerator division of CERN for the excellent performance of the LEP accelerator. Thanks are also due to the technical personnel of the collaborating institutions for their support in constructing and maintaining the ALEPH experiment. Those of us not from member states wish to thank CERN for its hospitality.

References

[1] ALEPH collaboration, D. Buskulic *et al.*, Z. Phys. **C62** (1994) 539.
DELPHI collaboration, P. Abreu *et al.*, Nucl. Phys. **B418** (1994) 403.
L3 collaboration, M. Acciarri *et al.*, Z. Phys. **C62** (1994) 551.
OPAL collaboration, R. Akers *et al.*, Z. Phys. **C61** (1994) 19.

[2] OPAL collaboration, P. Acton *et al.*, Phys. Lett. **B273** (1991) 338.
DELPHI collaboration, P. Abreu *et al.*, Z. Phys. **C65** (1995) 603.
L3 collaboration, M. Acciarri *et al.*, CERN-PPE/96-24 (February 1996), submitted to Phys. Lett. B

[3] R.G. Stuart, Phys. Lett. **B272** (1991) 353;
A. Leike, T. Riemann and J. Rose, Phys. Lett. **B273** (1991) 513.
T. Riemann, Phys.Lett. **B293** (1992) 451.

[4] J.E. Campagne and R. Zitoun, Z. Phys. **C43** (1989) 469; and Proc. of the Brighton Workshop on Radiative Corrections, Sussex, July 1989.

[5] S.Jadach, B.F.L. Ward and Z. Was, Comp. Phys. Comm. **79** (1994) 503.

[6] J-M Frere, V.A. Novikov and M.I. Vysotsky, *Zeroes of the process* $e^+e^- \to \bar{f}f$ *cross section and search for new physics*, ULB-TH/96-5, HEP-PH/9605241

[7] The S-matrix Subgroup of the LEP Electroweak Working Group, March 1996. ALEPH 96-044, PHYSIC 96-040.

[8] HRS Collab., M. Derrick *et al.*, Phys. Rev. **D31** (1985) 2352;
MAC Collab., W. W. Ash *et al.*, Phys. Rev. Lett. **55** (1985) 1831;
MARK II Collab., M. E. Levi *et al.*, Phys. Rev. Lett. **51** (1983) 1941;

[9] CELLO Collab., H. J. Behrend *et al.*, Phys. lett. **B191** (1987) 209;
JADE Collab., W. Bartel *et al.*, Z. Phys. **C26** (1985) 507;
MARK J Collab., B. Adeva *et al.*, Phys. Rev. **D38** (1988) 2665;
PLUTO Collab., Ch. Berger *et al.*, Z. Phys. **C21** (1983) 53;
TASSO Collab., W. Braunschweig *et al.*, Z. Phys. **C40** (1988) 163;

[10] AMY Collab., A. Bacala *et al.*, Phys. lett. **B331** (1994) 227;
TOPAZ Collab., B. Howell *et al.*, Phys. lett. **B291** (1992) 206;
VENUS Collab., K. Abe *et al.*, Z. Phys. **C48** (1990) 13;

[11] ALEPH Collab., *Preliminary results on Z production cross-sections and lepton forward-backward asymmetries using 1995 data.* Paper contributed to Warsaw conference, July (1996) PA07-069, and references therein.

[12] A. Leike, S. Riemman and T. Riemann, Munich University Preprint LMU-91/06, and FORTRAN program ZEFIT; and Phys. Lett. **B291** (1992) 187.

[13] CDF Collab., F. Abe *et al.*, Phys. Rev. **D51** (1995) 51;

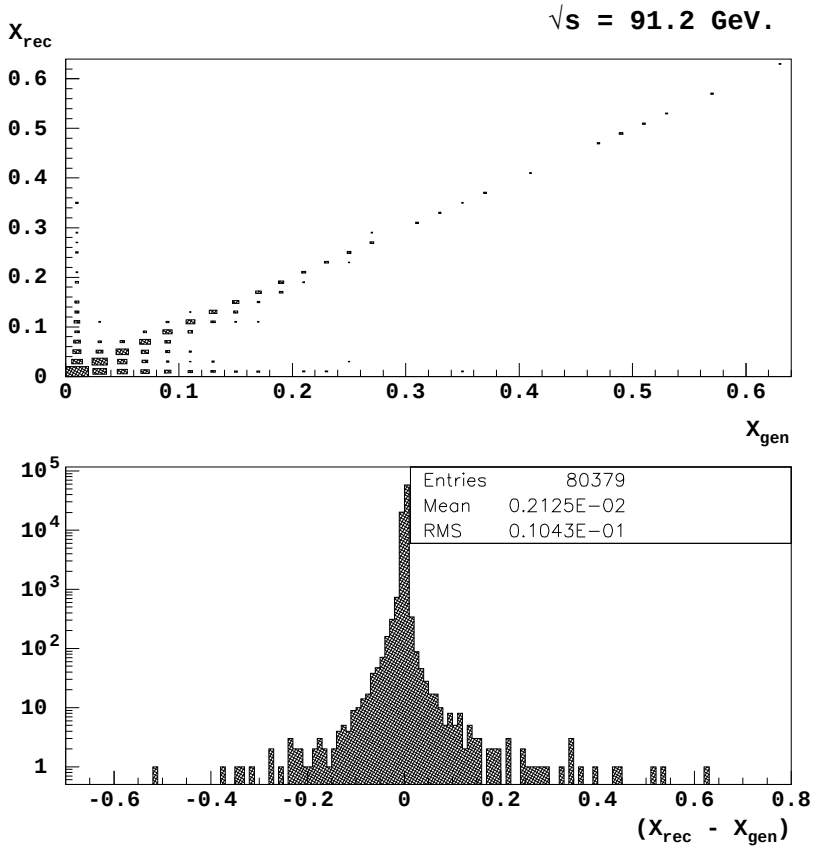

Figure 1: Monte Carlo study of the performance of the $s' \equiv s(1-x)$ reconstruction at $\sqrt{s} \sim 91.2$ GeV. The size of the squares is proportional to the logarithm of the number of events.

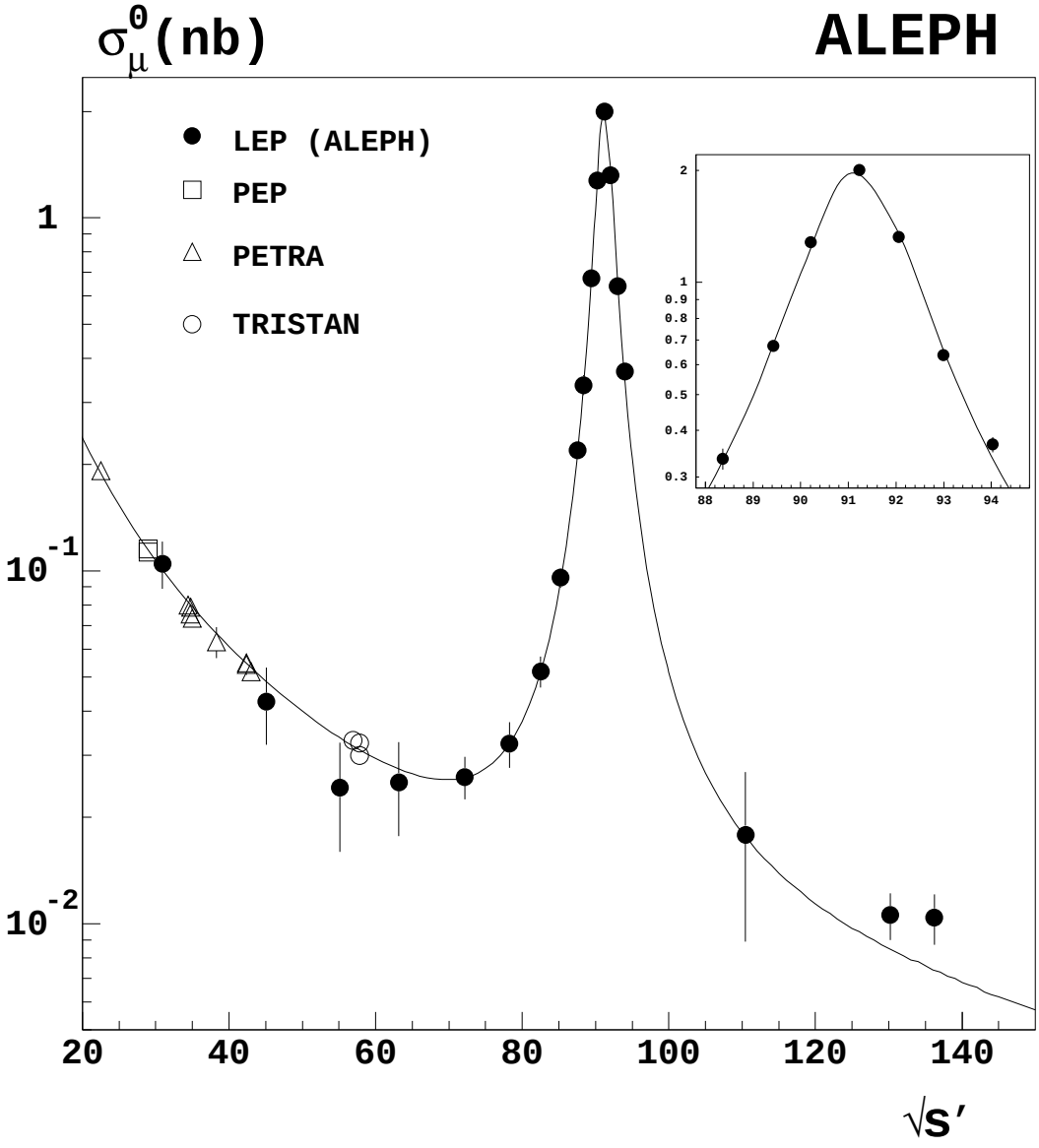

Figure 2: Measured cross-sections of muon-pair production compared with the fit results. The ALEPH measurements below 60 GeV correspond to the exclusive hard ISR selection that have not been used in the fit. For comparison the measurements at lower energies from PEP, PETRA and TRISTAN are included. The region around the Z pole has been amplified in the inserted box.

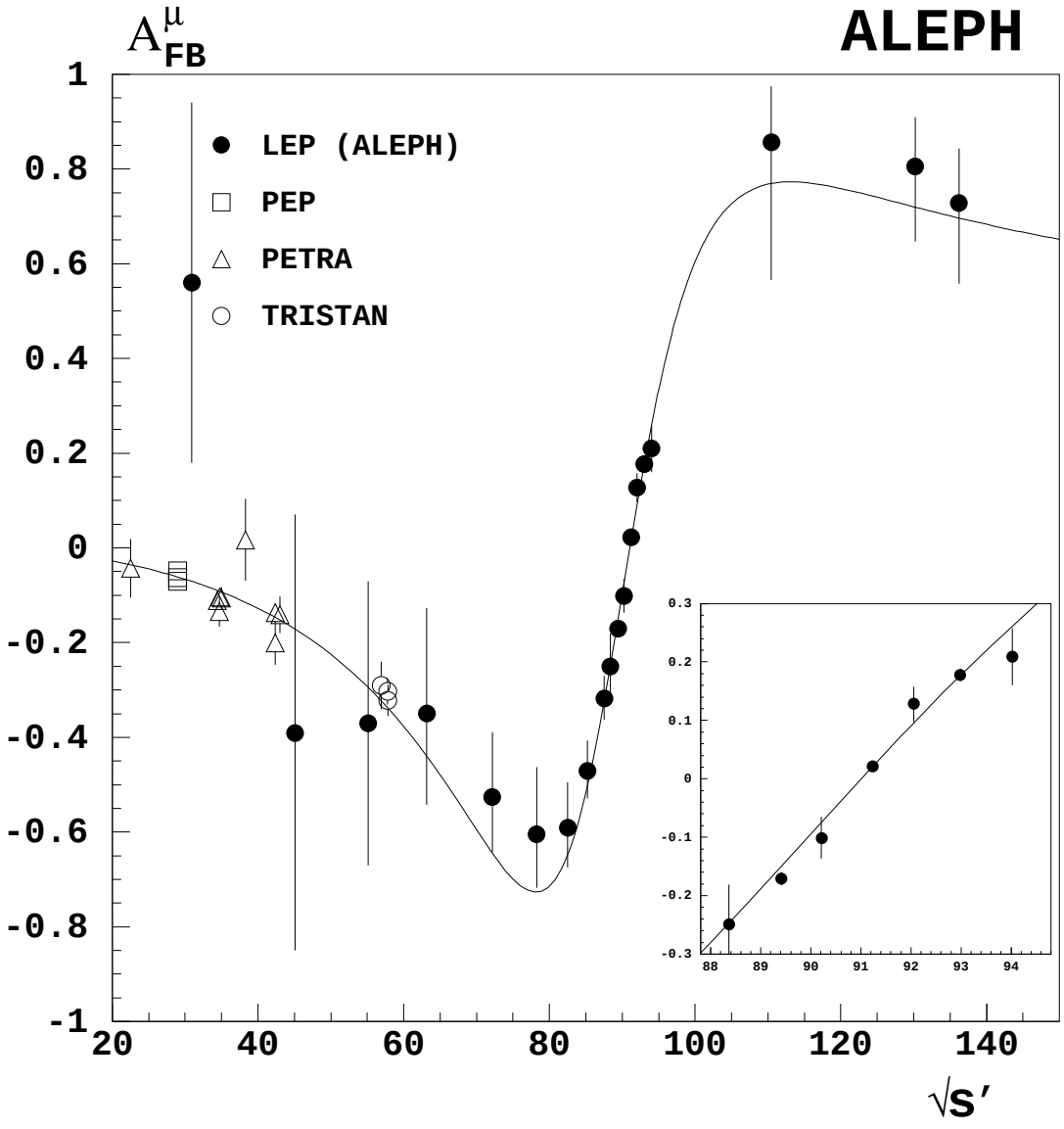

Figure 3: Measured forward-backward asymmetries of muon-pair production compared with the fit results. The ALEPH measurements below 60 GeV correspond to the exclusive hard ISR selection that have not been used in the fit. For comparison the measurements at lower energies from PEP, PETRA and TRISTAN are included. The region around the Z pole has been amplified in the inserted box.

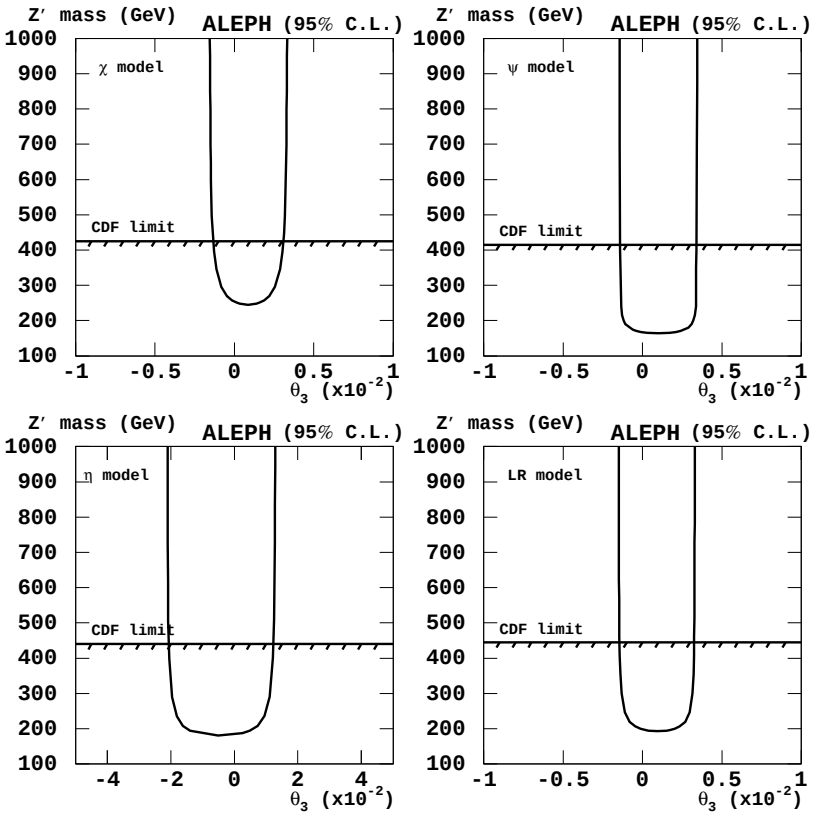

Figure 4: Curves corresponding to 95% confidence limits, dividing the $M_{Z'}$ - θ_3 plane into allowed and excluded regions.

Tables

$\sqrt{s'}$	C_1 (GeV)	C_2	C_3	C_4 (GeV)
$20-30$	20	1.0	0.60	10
$30-40$	15	0.2	0.60	8
$40-50$	10	0.2	0.94	6
$50-60$	8	0.1	0.94	5
$60-70$	6	0.05	0.94	5
$70-80$	3	0.03	0.94	5
$80-85$	2	0.02	0.94	5
$85-87$	2	0.02	0.94	5
$87-88$	2	0.02	0.94	5

Table 1: Cuts used to identify hard ISR events as a function of the reconstructed effective centre-of-mass energy.

$\sqrt{s'}$ GeV	$<\sqrt{s'}>$ GeV	N^{obs}	N^{MC}	Pull	$N_{2\gamma}$ Backg.
$20 \to 40$	30.94	56	54.6	+0.2	14.3
$40 \to 50$	45.11	28	31.0	-0.5	9.0
$50 \to 60$	55.12	17	23.8	-1.3	0.0
$60 \to 70$	65.15	33	36.1	-0.5	1.8
$70 \to 80$	76.08	77	74.9	+0.2	0.0
$80 \to 85$	83.37	167	167.3	0.0	0.0
$85 \to 87$	86.13	256	264.8	-0.5	0.0
$87 \to 88$	87.53	345	354.8	-0.5	0.0

Table 2: Number of observed hard ISR events in the different intervals of $\sqrt{s'}$ compared with the number of events predicted by the MC and the number of two photon background.

$\sqrt{s'}$ GeV	$<\sqrt{s'}>$ GeV	N_F^{obs}	N_F^{fit}	Pull	N_B^{obs}	N_B^{fit}	Pull
$55 \to 65$	63.12	11	10.3	+0.1	17	19. 8	-0.5
$65 \to 75$	72.18	22	16.4	+1.2	37	39. 6	-0.4
$75 \to 80$	78.29	17	11.7	+1.3	35	37. 6	-0.4
$80 \to 84$	82.50	26	22.2	+0.8	74	76. 2	-0.3
$84 \to 86$	85.20	70	63.3	+0.8	169	167. 0	+0.2
$86. \to 87.8$	87.49	160	151.6	+0.7	307	296. 2	+0.6
$87.8 \to 88.6$	88.37	89	88.1	+0.1	145	142. 7	+0.2
$88.6 \to 89.6$	89.42	3336	3398.6	-1.1	4683	4563. 9	+1.8
$89.6 \to 90.3$	90.21	376	376.5	+0.0	459	436. 1	+1.1
$90.3 \to 91.3$	91.23	55258	54872.8	+1.6	53974	53784. 4	+0.8
$91.3 \to 92.3$	92.05	619	612.2	+0.3	511	539. 7	-1.2
$92.3 \to 93.3$	92.99	5268	5393.1	-1.7	4036	4133. 4	-1.5
$93.3 \to 100$	94.03	247	236.2	+0.7	190	162. 5	+2.2
$100 \to 127$	110.46	12	11.3	+0.1	2	3. 2	-0.3
$127 \to 133$	130.20	32	24.4	+1.5	4	4. 6	0.0
$133 \to 136$	136.21	28	19.5	+1.9	5	4. 0	+0.3

Table 3: Number of observed events in the different intervals of $\sqrt{s'}$ for the inclusive analysis compared with the number of events predicted from the fit results.

	SM predictions	Fit results	Correlation matrix
r_μ^{tot}	0.14268	0.14201 $\pm$ 0.00084	1.00 0.06 0.04 0.12
j_μ^{tot}	0.004	-0.017 $\pm$ 0.020	1.00 -0.04 -0.33
r_μ^{fb}	0.00271	0.00272 $\pm$ 0.00054	1.00 0.12
j_μ^{fb}	0.799	0.804 $\pm$ 0.024	1.00

Table 4: Results obtained for the EW parameters from a maximum log-likelihood fit to the events selected in the inclusive analysis.

$<\sqrt{s'}>$ GeV	σ^0 (nb)	σ^{fit}	pull	A^0_{FB}	A^{fit}_{FB}	pull
30.94	0.105 ± 0.016	0.1007	+0.3	$+0.56 \pm 0.38$	-0.07	+1.7
45.11	0.043 ± 0.011	0.0484	-0.6	-0.39 ± 0.46	-0.17	-0.5
55.12	0.0243 ± 0.0083	0.0336	-1.1	-0.37 ± 0.30	-0.29	-0.3
65.15	0.0240 ± 0.0056	0.0265	-0.4	-0.44 ± 0.28	-0.48	+0.2
76.08	0.0285 ± 0.0034	0.0286	0.0	-0.52 ± 0.14	-0.71	+1.4
83.37	0.0600 ± 0.0047	0.0602	-0.1	-0.62 ± 0.08	-0.61	-0.1
86.13	0.1177 ± 0.0075	0.1226	-0.7	-0.28 ± 0.07	-0.44	+2.2
87.53	0.208 ± 0.011	0.2144	-0.5	-0.33 ± 0.06	-0.32	-0.1

Table 5: Measured cross-sections and asymmetries in the exclusive analysis compared with those predicted from the fit results.

$<\sqrt{s'}>$ GeV	σ^0 (nb)	σ^{fit}	pull	A^0_{FB}	A^{fit}_{FB}	pull
63.12	0.0252 ± 0.0075	0.0274	-0.3	$-0.35^{+0.22}_{-0.19}$	-.439	+0.5
72.18	0.0261 ± 0.0036	0.0259	+0.1	$-0.53^{+0.14}_{-0.12}$	-.645	+1.0
78.29	0.0324 ± 0.0048	0.0324	0.0	$-0.60^{+0.14}_{-0.11}$	-.727	+1.1
82.50	0.0519 ± 0.0052	0.0516	+0.1	$-0.591^{+0.096}_{-0.083}$	-.649	+0.7
85.20	0.0955 ± 0.0061	0.0922	+0.5	$-0.470^{+0.063}_{-0.059}$	-.503	+0.6
87.49	0.2192 ± 0.0099	0.2102	+0.9	$-0.317^{+0.047}_{-0.045}$	-.325	+0.2
88.37	0.336 ± 0.022	0.3317	+0.2	-0.250 ± 0.067	-.247	0.0
89.42	0.6734 ± 0.0075	0.6686	+0.6	-0.171 ± 0.011	-.149	-1.9
90.21	1.278 ± 0.044	1.2440	+0.8	-0.101 ± 0.036	-.074	-0.7
91.23	2.0011 ± 0.0060	1.9905	+1.7	0.0218 ± 0.0030	0.0200	+0.6
92.05	1.321 ± 0.040	1.3453	-0.6	0.128 ± 0.030	0.095	+1.1
92.99	0.6382 ± 0.0067	0.6535	-2.3	0.178 ± 0.010	0.177	0.0
94.03	0.367 ± 0.017	0.3362	+1.8	0.209 ± 0.049	0.262	-1.1
110.46	0.0179 ± 0.0090	0.0176	0.0	$0.86^{+0.12}_{-0.29}$	0.769	+0.3
130.20	0.0106 ± 0.0016	0.0085	+1.4	$0.80^{+0.10}_{-0.16}$	0.719	+0.5
136.21	0.0104 ± 0.0017	0.0074	+1.8	$0.73^{+0.13}_{-0.17}$	0.696	+0.2

Table 6: Measured cross-sections and asymmetries in the inclusive analysis compared with those predicted from the fit results.

Source of Syst.	Δr_μ^{tot}	Δj_μ^{tot}	Δr_μ^{fb}	Δj_μ^{fb}
MC statistics	0.00003	0.006	0. 00003	0.009
I-F QED interf.	0.00002	0.002	0. 00037	0.010
FSR	nil	0.003	0. 00005	0.004
Background	nil	0.001	0. 00002	0.003
$\Delta\sigma_{bs}$	0.00003	nil	nil	nil
TOTAL SYST.	0.00005	0.007	0. 00037	0.014

Table 7: Breakdown of the different contributions to the total systematic errors.

	$E_6(\chi)$	$E_6(\psi)$	$E_6(\eta)$	L-R(1.0)
$M_{Z'} >$	245. GeV	164. GeV	181. GeV	193.GeV
$\theta_3 >$	-0.0015	-0.0014	-0.021	-0.0015
$\theta_3 <$	+0.0033	+0.0034	+0.013	+0.0033

Table 8: 95% confidence limits on $M_{Z'}$ and θ_3 from fits to the predictions of several models.